Squeezing of electromagnetic field in a cavity by electrons in Trojan states

Piotr Kochański,[1,2,*] Zofia Bialynicka-Birula,[2,3] and Iwo Bialynicki-Birula[1,2,4,†]
[1]*Center for Theoretical Physics, Aleja Lotników 32/46, 02-668 Warsaw, Poland*
[2]*College of Science, Aleja Lotników 32/46, 02-668 Warsaw, Poland*
[3]*Institute of Physics, Aleja Lotników 32/46, 02-668 Warsaw, Poland*
[4]*Institute of Theoretical Physics, Warsaw University, 00-681 Warsaw, Poland*
(Received 12 July 2000; published 12 December 2000)

The notion of the Trojan state of a Rydberg electron, introduced by I. Bialynicki-Birula, M. Kaliński, and J. H. Eberly [Phys. Rev. Lett. **73**, 1777 (1994)] is extended to the case of an electromagnetic field quantized in a cavity. The shape of the electronic wave packet describing the Trojan state is practically the same as in the previously studied externally driven system. The fluctuations of the quantized electromagnetic field around its classical value exhibit strong squeezing. The emergence of Trojan states in the cylindrically symmetrical system is attributed to spontaneous symmetry breaking.

DOI: 10.1103/PhysRevA.63.013811 PACS number(s): 42.50.Ct, 32.80.−t

I. INTRODUCTION

The possibility of creating stationary, nondispersive, localized, wave packets describing a highly excited electron in a hydrogen atom strongly driven by circularly polarized microwave radiation was predicted theoretically several years ago [1], and confirmed in numerous publications [2–4] (for recent reviews of the subject, see Refs. [5–7]). Such electronic states are called Trojan wave packets, in analogy to the cloud of Trojan asteroid in the Sun-Jupiter system.

In all previous studies the microwave field was treated as an external, classical wave. Dressing of an electron by such a wave of a suitably chosen intensity, and a frequency equal to the Kepler frequency of the electron on the Rydberg orbit, makes the Trojan wave packets highly stable. Their lifetime is of the order of 1 sec [8,9], which makes them an interesting object of study for theoretical and perhaps even for practical reasons.

In the present paper a similar problem of nondispersive electronic wave packets is studied for an atom interacting with a *quantized* electromagnetic field. Such an approach allows for a fully dynamical treatment of an autonomous atom-field system. It automatically includes a back reaction of the atom on the electromagnetic field. Thus one can study both the dynamics and the statistical properties of the electromagnetic radiation. Our study fully confirms the existence of Trojan states of the Rydberg electron in this new regime, with almost exactly the same shape of the wave packet. The back reaction of the electron on the electromagnetic field pushes the field frequency off resonance. The quantum fluctuations of the electromagnetic field exhibit strong squeezing.

II. HYDROGEN ATOM IN A CAVITY

Anticipating the role of highly populated, discrete modes of the microwave field in the formation of Trojan electronic states, we consider a hydrogen atom in a microwave cavity. In the presence of a cavity we can separate a finite number of relevant degrees of freedom, whereas in free space we would have to deal with a continuous spectrum which precludes the existence of localized stationary states of the system.

To allow for the rotational symmetry of the atom-field system, we choose a cylindrical cavity. Its dimensions will be large enough to justify the dipole approximation in the coupling of hydrogen atom with the lowest cavity modes. The atom placed in the middle of cavity interacts only with TE_{1n} modes. For definitness we choose the two (degenerate) lowest modes of this type $(n=1)$ (labeled by X and Y), for which the mode functions have the forms

$$\mathbf{E}^X = i\mathcal{N}\omega \sin\frac{\pi z}{L}\,\mathbf{e}_z\times\boldsymbol{\nabla}_\perp J_1(x_{11}r/R)\sin\varphi, \tag{1a}$$

$$\mathbf{B}^X = -\frac{\mathcal{N}\pi}{L}\cos\frac{\pi z}{L}\,\boldsymbol{\nabla}_\perp J_1(x_{11}r/R)\sin\varphi, \tag{1b}$$

$$\mathbf{E}^Y = -i\mathcal{N}\omega \sin\frac{\pi z}{L}\,\mathbf{e}_z\times\boldsymbol{\nabla}_\perp J_1(x_{11}r/R)\cos\varphi, \tag{1c}$$

$$\mathbf{B}^Y = \frac{\mathcal{N}\pi}{L}\cos\frac{\pi z}{L}\,\nabla_\perp J_1(x_{11}r/R)\cos\varphi, \tag{1d}$$

where R and L are the radius and the length of the cavity, and x_{11} is the first (the smallest) solution of the equation $dJ_1(x)/dx=0$. The z axis is taken along the cylinder axis, and $\boldsymbol{\nabla}_\perp=(\partial/\partial x,\partial/\partial y)$. The frequency of the modes and the effective wave vector are given as

$$\omega = \frac{c}{R}[x_{11}^2+(\pi R/L)^2]^{1/2}, \tag{2}$$

$$k = \sqrt{(\omega/c)^2-(\pi/L)^2}. \tag{3}$$

The value of the normalization constant $\mathcal{N}$ was obtained in Ref. [10],

*Email address: piokoch@cft.edu.pl
†Email address: birula@cft.edu.pl

$$\mathcal{N}=\frac{x_{11}}{k^2R^2}\left(\frac{\hbar}{2\pi\epsilon_0 L\omega(1-1/x_{11}^2)J_1^2(x_{11})}\right)^{1/2}, \tag{4}$$

from the requirement that the energy per one photon in a mode is equal to $\hbar\omega$.

At the position $\mathbf{r}_A=(0,0,L/2)$ of the center of the atom, the orthogonal field vectors $\mathbf{E}^X$ and $\mathbf{E}^Y$ point in x and y directions, respectively, and are given by simple formulas:

$$\mathbf{E}^X(\mathbf{r}_A)=\frac{-i\mathcal{N}\omega x_{11}}{2R}\mathbf{e}_x, \tag{5a}$$

$$\mathbf{E}^Y(\mathbf{r}_A)=\frac{-i\mathcal{N}\omega x_{11}}{2R}\mathbf{e}_y, \tag{5b}$$

$$\mathbf{B}^X(\mathbf{r}_A)=0, \quad B^Y(\mathbf{r}_A)=0. \tag{5c}$$

The relevant part of the electric and magnetic field in the cavity can be written in the form

$$\mathbf{E}=\mathbf{E}^X a_X+\mathbf{E}^X{}^* a_X^*+\mathbf{E}^Y a_Y+\mathbf{E}^Y{}^* a_Y^*, \tag{6a}$$

$$\mathbf{B}=\mathbf{B}^X a_X+\mathbf{B}^X{}^* a_X^*+\mathbf{B}^Y a_Y+\mathbf{B}^Y{}^* a_Y^*, \tag{6b}$$

where a_X and a_Y are the dimensionless mode expansion amplitudes.

In the laboratory frame the dynamics of the atom-field system is governed by the Hamiltonian

$$H_L=\frac{\mathbf{p}^2}{2m}-\frac{e^2}{4\pi\epsilon_0 r}-e\mathbf{r}\cdot\mathbf{E}(\mathbf{r}_A)+\frac{1}{2}\int(\epsilon_0\mathbf{E}^2+\mathbf{B}^2/\mu_0)d^3\mathbf{r}, \tag{7}$$

where $\mathbf{r}=(x,y,z)$ is the position of the electron relative to the center of the atom $\mathbf{r}_A$. The Hamiltonian H_L describes the mutual interaction of the atomic electron with the chosen cavity modes. We can rewrite H_L using the amplitudes a_X and a_Y, or more conveniently, using their real combinations

$$P_x=\frac{-i}{\sqrt{2}}(a_X-a_X^*), \quad P_y=\frac{-i}{\sqrt{2}}(a_Y-a_Y^*), \tag{8a}$$

$$Q_x=\frac{1}{\sqrt{2}}(a_X+a_X^*), \quad Q_y=\frac{1}{\sqrt{2}}(a_Y+a_Y^*), \tag{8b}$$

where the dimensionless vectors $\mathbf{P}$ and $\mathbf{Q}$ represent the electric field and the magnetic induction:

$$H_L=\frac{\mathbf{p}^2}{2m}-\frac{e^2}{4\pi\epsilon_0 r}-e\mathcal{E}\mathbf{r}\cdot\mathbf{P}+\frac{\hbar\omega}{2}(\mathbf{P}^2+\mathbf{Q}^2). \tag{9}$$

The field amplitude $\mathcal{E}$ is

$$\mathcal{E}=\frac{\mathcal{N}\omega x_{11}}{R\sqrt{2}}. \tag{10}$$

We have found it convenient to use natural units for our problem derived from the field frequency for the energy, length, and momentum: $\hbar\omega$, $\sqrt{\hbar/m\omega}$, and $\sqrt{\hbar m\omega}$. The Hamiltonian [Eq. (9)] in these units takes on the form

$$H_L=\frac{\mathbf{p}^2}{2}-\frac{\tilde{q}}{r}-\gamma\mathbf{r}\cdot\mathbf{P}+\frac{\mathbf{P}^2+\mathbf{Q}^2}{2},$$

where the dimensionless parameters $\tilde{q}$ and γ characterizing the strength of the Coulomb field and the atom-field coupling are

$$\tilde{q}=\frac{e^2}{4\pi\epsilon_0\hbar\omega}\left(\frac{m\omega}{\hbar}\right)^{1/2}, \quad \gamma=\frac{e\mathcal{E}}{\hbar\omega}\left(\frac{\hbar}{m\omega}\right)^{1/2}. \tag{11}$$

III. CLASSICAL SOLUTIONS

We are interested in special solutions corresponding to Trojan states in the external electromagnetic wave introduced in Ref. [1]. Since these states describe electronic wave packets rotating around the nucleus along circular orbits, we transform the Hamiltonian H_L to the frame rotating around the z axis with the angular velocity Ω. The transformed Hamiltonian is

$$H=\frac{\mathbf{p}^2}{2}-\frac{\tilde{q}}{r}-\gamma\mathbf{r}\cdot\mathbf{P}+\frac{\mathbf{P}^2+\mathbf{Q}^2}{2}-\kappa(M_z^A+M_z^F), \tag{12}$$

where $\kappa=\Omega/\omega$. The z components of the angular momenta of the electron and of the electromagnetic field are $M_z^A=xp_y-yp_x$ and $M_z^F=(Q_xP_y-Q_yP_x)$. In this frame, the rotational states will appear as stationary states of the Hamiltonian. We would like to stress that the Hamiltonian H cannot be identified with the energy because of the appearance of the inertial forces in the rotating frame.

To emphasize the rotational symmetry of our problem, we introduce the following variables for the electromagnetic field:

$$Q_+=\frac{Q_x-P_y}{\sqrt{2}}, \quad Q_-=\frac{Q_x+P_y}{\sqrt{2}}, \tag{13a}$$

$$P_+=\frac{Q_y+P_x}{\sqrt{2}}, \quad P_-=\frac{P_x-Q_y}{\sqrt{2}}, \tag{13b}$$

corresponding to the left and right circular polarizations. In terms of these variables the Hamiltonian takes on the form

$$H=\frac{\mathbf{p}^2}{2}-\frac{\tilde{q}}{r}-\frac{\gamma}{\sqrt{2}}[x(P_++P_-)+y(Q_--Q_+)]+\frac{1+\kappa}{2}(P_+^2+Q_+^2)+\frac{1-\kappa}{2}(P_-^2+Q_-^2)-\kappa M_z^A. \tag{14}$$

The kinetic part of the field Hamiltonian is made up of two terms: corotating and counter-rotating. Linear stability analysis shows that both parts are necessary for the existence of the nontrivial equilibrium solution. From Hamiltonian (12), we derive the evolution equations

$$\dot{x}=p_x+\kappa y, \tag{15a}$$

$$\dot{y}=p_y-\kappa x, \tag{15b}$$

$$\dot{z}=p_x, \tag{15c}$$

$$\dot{Q}_+=(1+\kappa)P_+-\gamma x/\sqrt{2}, \tag{15d}$$

$$\dot{Q}_-=(1-\kappa)P_--\gamma x/\sqrt{2}, \tag{15e}$$

$$\dot{p}_x=-\frac{\tilde{q}x}{r^3}+\frac{\gamma(P_++P_-)}{\sqrt{2}}+\kappa p_y, \tag{15f}$$

$$\dot{p}_y=-\frac{\tilde{q}y}{r^3}+\frac{\gamma(Q_--Q_+)}{\sqrt{2}}-\kappa p_x, \tag{15g}$$

$$\dot{p}_z=-\frac{\tilde{q}z}{r^3}, \tag{15h}$$

$$\dot{P}_+=-(1+\kappa)Q_+-\gamma y/\sqrt{2}, \tag{15i}$$

$$\dot{P}_-=-(1-\kappa)Q_-+\gamma y/\sqrt{2}. \tag{15j}$$

The time-independent solutions of these equations describe the stationary states of our system. Equating the left-hand side of Eqs. (15]) to zero, we obtain

$$x^{\mathrm{eq}}=r_0\cos\varphi, \quad y^{\mathrm{eq}}=r_0\sin\varphi, \quad z^{\mathrm{eq}}=0, \tag{16a}$$

$$p_x^{\mathrm{eq}}=-\kappa r_0\sin\varphi, \quad p_g^{\mathrm{eq}}=\kappa r_0\cos\varphi, \quad p_z^{\mathrm{eq}}=0, \tag{16b}$$

$$Q_+^{\mathrm{eq}}=\frac{-\gamma r_0\sin\varphi}{(\kappa+1)\sqrt{2}}, \quad Q_-^{\mathrm{eq}}=\frac{-\gamma r_0\sin\varphi}{(\kappa-1)\sqrt{2}}, \tag{16c}$$

$$P_+^{\mathrm{eq}}=\frac{\gamma r_0\cos\varphi}{(\kappa+1)\sqrt{2}}, \quad P_-^{\mathrm{eq}}=\frac{-\gamma r_0\cos\varphi}{(\kappa-1)\sqrt{2}}. \tag{16d}$$

In addition, Eqs. (15f) and (15g) give the equilibrium condition

$$\frac{\tilde{q}}{r_0^3}=\kappa^2-\frac{\gamma^2}{\kappa^2-1}. \tag{17}$$

This equilibrium condition can be used to express the equilibrium radius r_0 in terms of the frequency of the cavity mode ω and the frequency of rotation Ω,

$$r_0(\Omega)=\tilde{q}^{1/3}\left((\Omega/\omega)^2-\frac{\gamma^2}{(\Omega/\omega)^2-1}\right)^{-1/3}, \tag{18}$$

or, alternatively, to express the frequency of rotation in terms of ω and r_0. The equilibrium condition [Eq. (17)] has two solutions for Ω, denoted by $\Omega^{>}(r_0)$ and $\Omega^{<}(r_0)$:

$$\Omega^{>}(r_0)=\frac{\omega}{\sqrt{2}}\sqrt{1+\tilde{q}/r_0^3+\sqrt{(1-\tilde{q}/r_0^3)^2+4\gamma^2}}, \tag{19a}$$

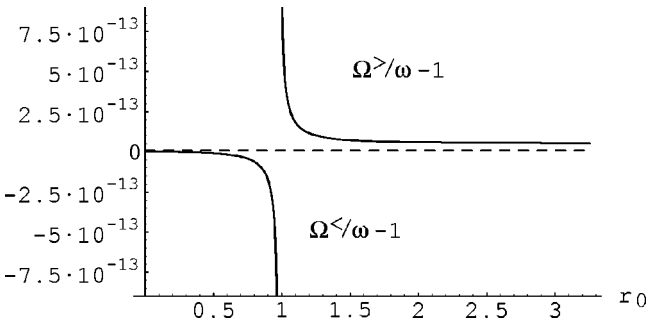

FIG. 1. Two branches of the frequency of rotation $\Omega(r_0)$. The upper curve corresponds to the Trojan states, and the lower curve corresponds to the anti-Trojan states; r_0 is measured in units of $3600a_0$ (a_0 is the atom Bohr radius).

$$\Omega^{<}(r_0)=\frac{\omega}{\sqrt{2}}\sqrt{1+\tilde{q}/r_0^3-\sqrt{(1-\tilde{q}/r_0^3)^2+4\gamma^2}}. \tag{19b}$$

Both solutions exist for all values of r_0. The solution $\Omega^{>}(r_0)[\Omega^{>}(r_0)]$ gives the frequency that is always higher (lower) than the cavity frequency ω (see Fig. 1). The higher frequency (larger centrifugal force) requires the electric field to be directed toward the nucleus, whereas the lower frequency requires the field to point outward. The first case corresponds to the Trojan states, and the second to the so-called anti-Trojan states. In a previous study [11,12], where the electromagnetic field was treated as a given external wave, the anti-Trojan states were found to be classically unstable. The classical stability obtained in the present study is due to detuning from the exact resonance. Since the localization of the electronic wave packet is much worse for the anti-Trojan states (classically, the trajectories in the rotating frame are spread almost evenly around the whole circle, cf.

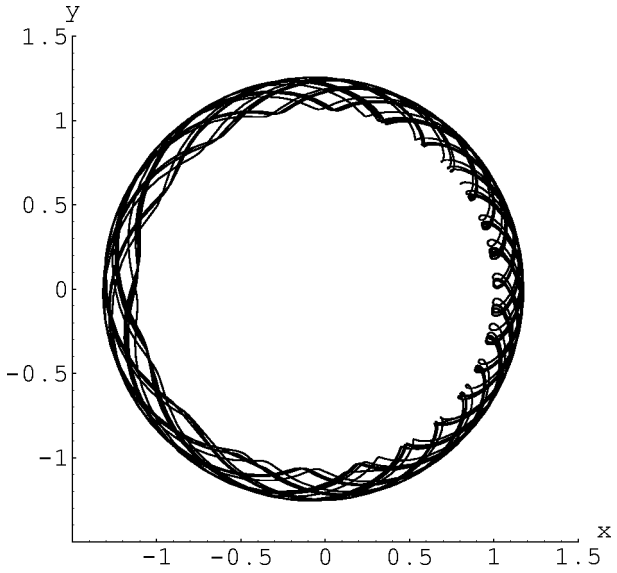

FIG. 2. A typical classical trajectory in the rotating frame near the anti-Trojan equilibrium position. The motion extends almost uniformly over the whole circle, but the electron spends a little more time in the right half of the circle.

Fig. 2), we will restrict ourselves to the Trojan states only. Hence, in what follows, we shall only consider the solution $\Omega^{>}(r_0)$.

Note, that for $\omega=\Omega$ (i.e., $\kappa=1$), we have only a trivial result $\mathbf{r}^{\mathrm{eq}}=\mathbf{p}^{\mathrm{eq}}=\mathbf{P}^{\mathrm{eq}}=\mathbf{Q}^{\mathrm{eq}}=\mathbf{0}$ which, in the classical model of an atom, means that ''the electron has fallen onto the nucleus'' and the electric field is zero. Thus, every nontrivial solution requires the presence of a detuning ($\omega\neq\Omega$) between the cavity frequency and the Kepler frequency. This phenomenon is known as frequency pushing, and is a direct consequence of the mutual atom-field interaction. This detuning was absent in all previous approaches where the atom was driven by an external wave.

Equation (15) have a continuum of time-independent solutions that can be labeled by r_0 and an angle φ in the *x*-*y* plane. In the laboratory frame these solutions describe a classical electron circulating around the nucleus at the distance r_0. The orbit of the electron is confined to the *x*-*y* plane. The electron is dressed by the classical electromagnetic field

$$\mathbf{E}=-\frac{\mathcal{E}\sqrt{2}}{\kappa^2-1}\frac{e\mathcal{E}r_0}{\hbar\omega}(\sin\varphi\mathbf{e}_y+\cos\varphi\mathbf{e}_x), \tag{20}$$

which has a resonance dependence on the parameter κ. Note that the electric field changes its sign when the frequency of rotation passes through the resonance.

Next we expand the Hamiltonian around a time-independent solution, and investigate its linear stability. The motion will be stable if all eigenfrequencies are real. The characteristic equation for this problem has the form

$$\begin{aligned}\lambda^2(\lambda^2-q_r)[\lambda^6-(4+q_r+2)\Gamma]\lambda^4+\{5-3/5q_r+q_r^2/2+4\gamma^2\\ +(4+5/2q_r\Gamma)\lambda^2-[2+5/2q_r-5q_r^2+q_r^3+8\gamma^2\\ +14q_r\gamma^2+(2+7/2q_r+q_r^2/2+8\gamma^2)\Gamma]\}=0,\end{aligned} \tag{21}$$

where $q_r=\tilde{q}/r_0^3$ and $\Gamma=\sqrt{1-2q+q^2+4\gamma^2}$. The first ($\lambda=0$) frequency in our problem corresponds to the rotation of the whole system, and it is a reflection of the rotational symmetry. The second frequency ($\lambda=\sqrt{\tilde{q}/r_0^3}$) corresponds to the motion in the *z* direction that (in the linear approximation) is decoupled from the motion in the *x*-*y* plane. The remaining three frequencies correspond to the motion of the electron coupled to the electromagnetic field. We shall not produce the analytical expressions for these eigenfrequencies, but in Fig. 3 we plot the region of stability in the R-r_0 plane.

The stability can also be studied numerically, and calculations of the classical trajectories fully confirm the stability of the equilibrium solution. In Fig. 4 we plot the projection of a typical electron trajectory on the *x*-*y* plane for the time interval $(1400T,1500T)$, where $T=1/\omega$. The trajectory started at the equilibrium position $\mathbf{r}=r_0(1,0,0)$, with the initial momenta $\mathbf{p}=m\omega r_0(0.02,\kappa+0.07,0.02)$. As we see, the electron follows a rather complicated, but bounded, trajectory. Obviously, if we choose $p(t=0)$ sufficiently large, the electron will eventually leave the vicinity of the equilibrium point. In Fig. 5 we show the z-p_z cross section of the phase space for the same trajectory. This phase-space trajectory resembles the trajectory of a simple harmonic oscillator. In-

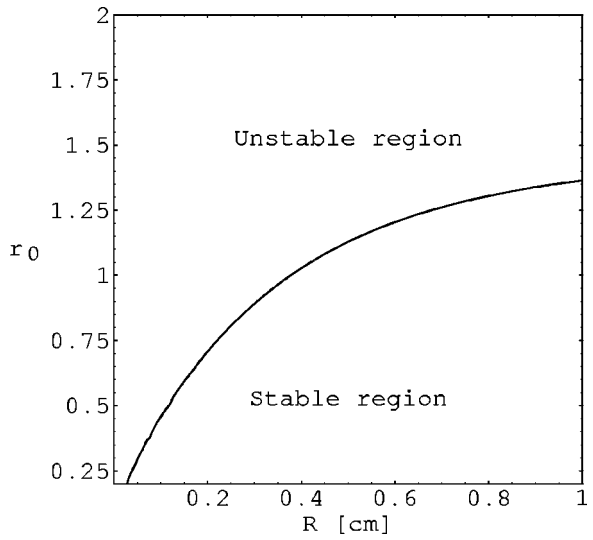

FIG. 3. The boundary between the stable and unstable regions of classical equilibrium; r_0 is measured in units of $3600a_0$ (a_0 is the atom Bohr radius).

deed, as we have seen in linearized evolution equations, the motion in the *z* direction is purely harmonic. Thus the interesting dynamics of the electron is found in the motion confined to the *x*-*y* plane, and in what follows we shall treat our problem as two dimensional.

Since our system is conservative, it has a well-defined energy H_L. We have calculated its value $E(\kappa)$ for all solutions that in the rotating frame are determined by Eqs. (16). This energy is given by the formula

$$E(\kappa)=\frac{m\omega^2r_0^2(\kappa)}{2}\left(\frac{\gamma^2}{(\kappa^2-1)^2}(5\kappa^2-3)-\kappa^2\right), \tag{22}$$

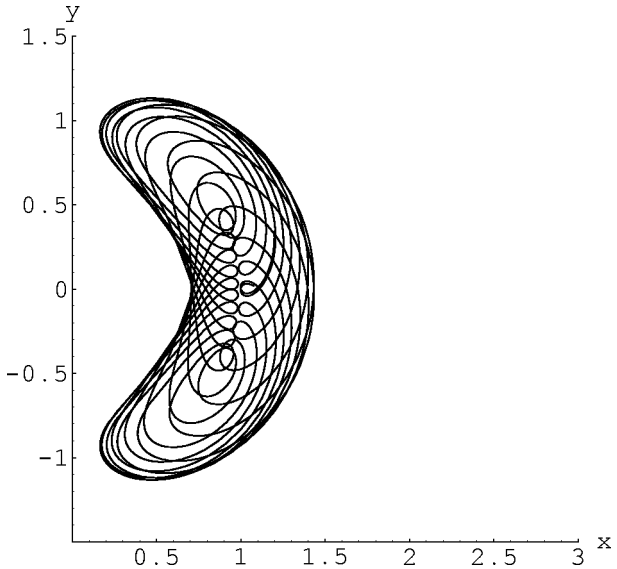

FIG. 4. Classical electron trajectory projected into the *x*-*y* plane; *x* and *y* are measured in units of r_0. The trajectory started at time $t=0$ from equilibrium position (16), with the initial momenta $\mathbf{p}=m\omega r_0(0.02,\kappa+0.07,0.02)$, and is plotted for the time interval $(1400T,1500T)$.

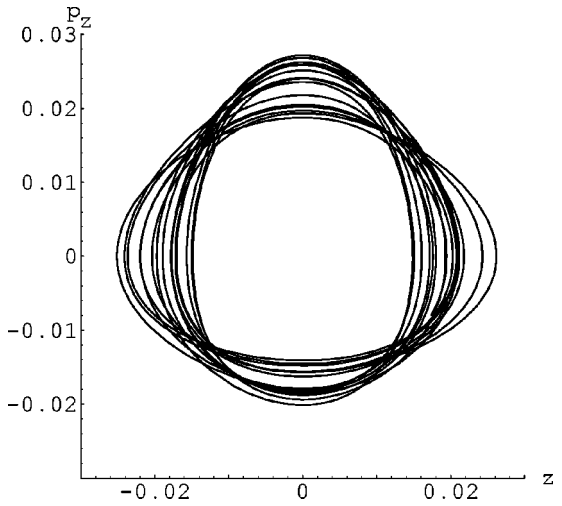

FIG. 5. Classical motion of the electron projected into the phase space z-p_z; z is measured in units of r_0, and p_z is measured in units of $m\omega r_0$. The trajectory started at time $t=0$ from equilibrium position (16) with the initial momenta $\mathbf{p}=m\omega r_0$ $(0.02,\kappa+0.07,0.02)$, and is plotted for the time interval $(1400T,1500T)$.

and is plotted in Fig. 6 as a function of κ. The infinite growth of the energy near the resonance ($\kappa=1$) expresses the phenomenon of the frequency pushing.

IV. QUANTUM EFFECTS

In order to study the quantum effects for the electron as well as for the electromagnetic field, we will apply the procedure of the quantization around the classical solutions [Eqs. (16)]. A similar quantization method was used before, for example, in nonlinear optics to describe quantum fluctuations around the classical solitons in fibers [13]. Here the quantization will lead to a description of the electron in terms of a quantum-mechanical wave packet orbiting along the classical trajectory and, at the same time, will reveal quantum fluctuations of the electromagnetic field around its classical value.

As a starting point we choose Hamiltonian (14), in which all variables are treated as operators and we express them as sums of their classical parts and the quantum corrections $\hat{\mathbf{r}}=\mathbf{r}^{\mathrm{eq}}+\mathbf{r}$, $\hat{\mathbf{p}}=\mathbf{p}^{\mathrm{eq}}+\mathbf{p}$, $\hat{\mathbf{Q}}=\mathbf{Q}^{\mathrm{eq}}+\mathbf{Q}$, and $\hat{\mathbf{P}}=\mathbf{P}^{\mathrm{eq}}+\mathbf{P}$. The classical parts represent equilibrium solutions [Eqs. (16)] found in Sec. III. In order to simplify the notation, we have not attached any labels to the operators of quantum corrections $(\mathbf{r},\mathbf{p},\mathbf{Q},P)$. Next we expand the Hamiltonian around the classical equilibrium solution, neglecting all terms higher than quadratic in the quantum corrections. To proceed along these lines, we have to choose one solution, labeled by φ_0, from the whole family of equilibrium solutions. Making this choice, we break the rotational symmetry of the Hamiltonian.

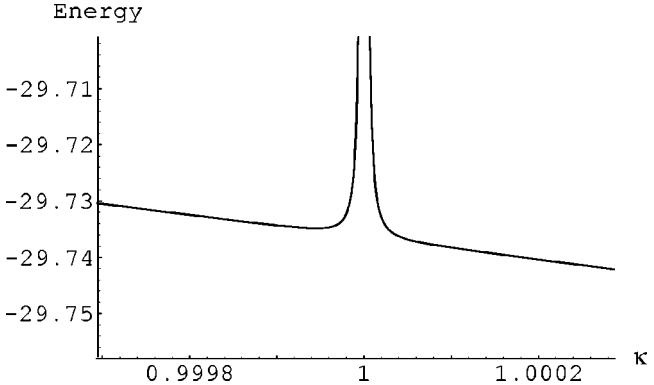

FIG. 6. The energy $E(\kappa)$ plotted in units of $\hbar\omega$.

This mechanism of selection of a specific classical solution resembles spontaneous symmetry breaking. Spontaneous symmetry breaking is present in many branches of physics. It explains the appearance of deformed nuclei, the formation of magnetic domains in ferromagnetic materials, or the emergence of Higgs particles in the Glashow-Weinberg-Salam model of electroweak interactions. In all these cases the symmetry is broken by the choice of a particular ground state. In our case, however, we do not break the symmetry by choosing a ground state but by choosing an equilibrium state of the Hamiltonian that is very far from the ground state of the system.

Once we have chosen some φ_0, we can rotate the frame of reference, so that the direction given by φ_0 is along the x axis. The quadratic Hamiltonian is

$$H_Q=\frac{\mathbf{p}^2}{2}-\frac{\gamma}{\sqrt{2}}[x(P_+ +P_-)+y(Q_- -Q_+)] + \frac{1+\kappa}{2}(P_+^2+Q_+^2)+\frac{1-\kappa}{2}(P_-^2+Q_-^2)-q\kappa^2x^2 + \frac{q\kappa^2y^2}{2}+\frac{q\kappa^2z^2}{2}-\kappa(xp_y-xp_x), \tag{23}$$

where the parameter q, the ratio of the Coulomb force to the centrifugal force,

$$q=\frac{e^2}{4\pi\epsilon_0 m r_0^3\Omega^2}=\frac{\tilde{q}}{r_0^3\kappa^2}, \tag{24}$$

has been introduced to achieve the full correspondence with the notation used before [1,14] in the description of Trojan states. Note that in this Hamiltonian the quadratic term $q\kappa^2x^2$ enters with a negative coefficient. If it were not for the rotational term, such a Hamiltonian would not have any stable points. In our case, however, the stability can be achieved for a particular choice of γ, q, and κ.

We look for a fundamental solution of the Schrödinger equation with the Hamiltonian H_Q in the form of a four-dimensional Gaussian function:

$$\psi=N\exp(-\tfrac{1}{2}\mathbf{X}\cdot A\cdot\mathbf{X}). \tag{25}$$

$\mathbf{X}=(x,y,Q_+,Q_-)$, and

$$A=\begin{pmatrix} a_{11} & ia_{12} & ia_{13} & ia_{14} \\ ia_{12} & a_{22} & a_{23} & a_{24} \\ ia_{13} & a_{23} & a_{33} & a_{34} \\ ia_{14} & a_{23} & a_{34} & a_{44} \end{pmatrix}. \tag{26}$$

Inserting this ansatz into the Schrödinger equation, we obtain ten algebraic, nonlinear equations for the parameters a_{ij}:

$$-2\kappa^2 q - a_{11}^2 + 2\kappa a_{12} + a_{12}^2 - 2\gamma a_{13} + a_{13}^2(1+\kappa) - 2\gamma a_{14} + a_{14}^2(1-\kappa) = 0, \tag{27a}$$

$$a_{11}a_{12} + a_{12}a_{22} - \gamma a_{23} + a_{13}a_{23} - \gamma a_{24} + a_{14}a_{24} + \kappa(-a_{11} + a_{22} + a_{13}a_{23} - a_{14}a_{24}) = 0, \tag{27b}$$

$$a_{11}a_{13} + a_{12}a_{23} - \gamma a_{33} + a_{13}a_{33} - \gamma a_{34} + a_{14}a_{34} + \kappa(a_{23} + a_{13}a_{33} - a_{14}a_{34}) = 0, \tag{27c}$$

$$a_{11}a_{14} + a_{12}a_{24} - \gamma a_{34} + a_{13}a_{34} - \gamma a_{44} + a_{14}a_{44} + \kappa(a_{24} + a_{13}a_{34} - a_{14}a_{44}) = 0, \tag{27d}$$

$$\kappa^2 q - 2\kappa a_{12} + a_{12}^2 - a_{22}^2 - a_{23}^2(1+\kappa) - a_{24}^2(1-\kappa) = 0, \tag{27e}$$

$$-\gamma - \kappa a_{13} + a_{12}a_{13} - a_{22}a_{23} - a_{23}a_{33} - \kappa a_{23}a_{33} - a_{24}a_{34} + \kappa a_{24}a_{34} = 0, \tag{27f}$$

$$\gamma - \kappa a_{14} + a_{12}a_{14} - a_{22}a_{24} - a_{23}a_{34} - \kappa a_{23}a_{34} - a_{24}a_{44} + \kappa a_{24}a_{44} = 0, \tag{27g}$$

$$1 + \kappa + a_{13}^2 - a_{23}^2 - a_{33}^2(1+\kappa) - a_{34}^2(1-\kappa) = 0, \tag{27h}$$

$$a_{13}a_{14} - a_{23}a_{24} - a_{34}((1+\kappa)a_{33} - (-1+\kappa)a_{44}) = 0, \tag{27i}$$

$$1 - \kappa + a_{14}^2 - a_{24}^2 - a_{44}^2(1-\kappa) - a_{34}^2(1+\kappa) = 0. \tag{27j}$$

We can easily solve these equations numerically, but first we want to find a perturbative solution. In order to do this we write the coupling constant in the form $\gamma = \overline{\gamma}\sqrt{\kappa - 1}$. Obviously $\overline{\gamma} = \sqrt{(1-q)(\kappa+1)}$, and we will treat $\overline{\gamma}$ as a small parameter. Typical values of the parameters are $\kappa = 1.000\,000\,1$ and $q = 0.956\,25$ which give $\overline{\gamma} = 0.06$. One can ask why we can not treat γ (or even simpler, $\kappa - 1$) as a perturbation parameter. However, if we do so, we face a problem: the coefficients of the perturbation series are growing, since they behave as $1/\sqrt{\kappa - 1}$. When we tend with $\kappa - 1$ to zero we hit exactly the resonance point, and the perturbation expansion becomes meaningless. On the other hand, when $\overline{\gamma}$ is chosen as an expansion parameter, all large contributions to the coefficients in the perturbation expansion $a_{ij} = a_{ij}^{(0)} + \overline{\gamma} a_{ij}^{(1)} + \overline{\gamma}^2 a_{ij}^{(2)} + \cdots$ cancel out.

TABLE I. Coefficients characterizing the fundamental state of the atom-field system calculated up to the second order of perturbation theory.

$a_{11} = 0.511\,60$	$a_{12} = 0.781\,64$	$a_{22} = 0.062\,70$
$a_{33} = 1$	$a_{34} = 1.49 \times 10^{-12}$	$a_{44} = 0.507\,51$
$a_{13} = 7.50 \times 10^{-7}$	$a_{14} = 4.50 \times 10^{-6}$	
$a_{23} = -5.33 \times 10^{-7}$	$a_{24} = -7.68 \times 10^{-7}$	

We analytically calculated the coefficients up to the second order, but here we present the analytic formulas only in zeroth order, and numerical values of the first- and second-order corrections

$$a_{11}^{(0)} = \kappa\left(\frac{(1+2q)[4g - 9q + 8 - 8s(q)]}{9q^2}\right)^{1/2}, \tag{28a}$$

$$a_{12}^{(0)} = \kappa\frac{2 + q - 2s(q)}{3q}, \tag{28b}$$

$$a_{22}^{(0)} = \kappa\left(\frac{(1-q)[4q - 9q + 8 - 8s(q)]}{9q}\right)^{1/2}, \tag{28c}$$

where $s(q) = \sqrt{1 + q - 2q}$,

$$a_{13}^{(0)} = 0, \quad a_{23}^{(0)} = 0, \quad a_{14}^{(0)} = 0, \quad a_{24}^{(0)} = 0, \quad a_{33}^{(0)} = 1, \quad a_{34}^{(0)} = 0, \quad a_{44}^{(0)} = 1. \tag{29}$$

Thus, in zeroth order, the electronic part of the wave packet is exactly the same as in the case of externally driven Trojan wave packet [1]. The electromagnetic part has the form of a coherent (nonsqueezed) state.

Higher corrections are due to the mutual interaction between the field and the atom. Numerical values of the parameters a_{ij} are calculated for the cavity parameters $L = 1$ cm and $R = 0.32$ cm, which give $\omega = 197$ GHz and $\gamma = 3.24 \times 10^{-7}$. The detuning κ is chosen in such a way that the value of q is optimal, $q = 0.956\,25$. As shown in Ref. [1], the wave packet is then maximally concentrated around the equilibrium point, and its center is located at $r_0 = 3600 a_0$ (a_0 is the atom Bohr radius). The expansion coefficients calculated up to the second order are presented in Table I. In this order we observe the effect of the back reaction of the electron on the electromagnetic field. However, the coefficients a_{11}, a_{12}, and a_{22}, characterizing the shape of the electronic wave packet, are the same as in zeroth order within the assumed accuracy.

In Table II we present the results of a direct numerical solution of our set of equations. As we see, almost all the

TABLE II. Coefficients characterizing the fundamental state of the atom-field system calculated numerically.

$a_{11} = 0.511\,60$	$a_{12} = 0.781\,64$	$a_{22} = 0.062\,70$
$a_{33} = 1$	$a_{34} = 1.40 \times 10^{-12}$	$a_{44} = 0.005\,32$
$a_{13} = 7.50 \times 10^{-7}$	$a_{14} = 4.668 \times 10^{-6}$	
$a_{23} = -5.33 \times 10^{-7}$	$a_{24} = -1.34 \times 10^{-6}$	

TABLE III. Correlations of positions and momenta for the electronic variables calculated in the fundamental state of the atom-field system. The position variables are measured in units of the electron orbit radius r_0, and the momenta are measured in the corresponding unit $m\Omega r_0$.

$\langle xx\rangle = 0.015\,95$	$\langle xp_x + p_x x\rangle = 0$
$\langle yy\rangle = 0.130\,14$	$\langle yp_y + p_y y\rangle = 0$
$\langle p_x p_x\rangle = 0.083\,69$	$\langle xp_y + p_y x\rangle = -0.024\,93$
$\langle p_y p_y\rangle = 0.010\,26$	$\langle yp_x + p_x y\rangle = -0.203\,45$
$\langle xy\rangle = 0$	$\langle p_x p_y\rangle = 0$

coefficients were already obtained correctly in the second order of perturbation theory. Only a_{44} differs from the exact numerical solution. This can be attributed to the very slowly convergent perturbation series for this particular coefficient. The coefficients a_{13}, a_{23}, a_{14}, and a_{24}, describing the mixing of the atomic part of the wave packet with the field part, are not zero. Moreover, the electromagnetic field is strongly affected by the interaction with the atom; the coefficient a_{44} is significantly different from its value in zeroth order.

The four-dimensional Gaussian wave packet [Eq. (25)], with the coefficients a_{ij} calculated numerically, describes the fundamental state of the mutually interacting atom-field system. Owing to its Gaussian form, this state saturates the multidimensional generalized uncertainty relations for the complete atom-field system (see Ref. [15]). The smallness of the coefficients a_{13}, a_{23}, a_{14}, and a_{24} expresses the fact that the field and the atom are only very weakly correlated in this state. As a result of this, the saturation of the uncertainty relations is almost exact, separately for both parts of the wave function. The average values of second moments the electronic variables calculated with the numerical values of the coefficients taken from Table II are given in Table III. This table exhibits the existence of correlations between the variables in the x and y directions. This requires the use of generalized uncertainty relations for a two-dimensional system in the form (cf. Ref. [15])

$$\langle xx\rangle\langle p_x p_x\rangle + \langle xy\rangle\langle p_x p_y\rangle - \frac{1}{4}(\langle xp_x + p_x x\rangle^2 + \langle xp_y + p_y x\rangle \times \langle p_x y + y p_x\rangle) \geqslant \frac{\hbar^2}{4}, \tag{30}$$

$$\langle yy\rangle\langle p_y p_y\rangle + \langle xy\rangle\langle p_x p_y\rangle - \frac{1}{4}(\langle yp_y + p_y y\rangle^2 + \langle yp_x + p_x y\rangle \times \langle p_y x + x p_y\rangle) \geqslant \frac{\hbar^2}{4}. \tag{31}$$

TABLE IV. Correlations of the electromagnetic field variables calculated in the fundamental state of the atom-field system.

$\langle Q_+ Q_+\rangle = 0.5$	$\langle (Q_+ P_+ + P_+ Q_+)\rangle = 0$
$\langle Q_- Q_-\rangle = 94.059\,00$	$\langle (Q_- P_- + P_- Q_-)\rangle = 0$
$\langle P_+ P_+\rangle = 0.5$	$\langle (Q_+ P_- + P_- Q_+)\rangle = 0$
$\langle P_- P_-\rangle = 0.002\,657$	$\langle (Q_- P_+ + P_+ Q_-)\rangle = 0$
$\langle Q_+ Q_-\rangle = 9.381\,13 \times 10^{-10}$	$\langle P_+ P_-\rangle = 4.121\,31 \times 10^{-12}$

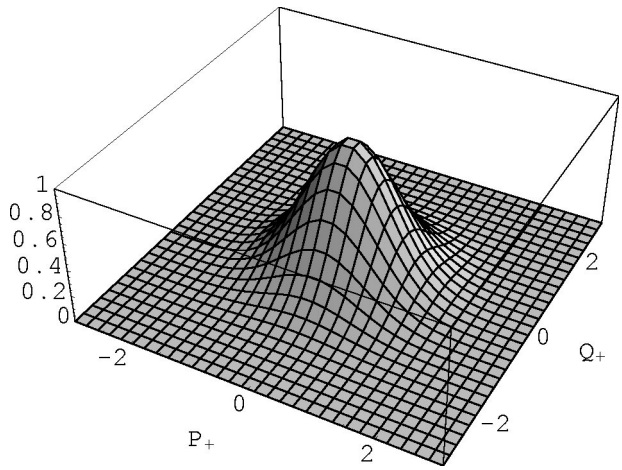

FIG. 7. The $Q_+ - P_+$ cross section of the Wigner function. In this (counter-rotating) mode the fluctuations of the electromagnetic radiation are not squeezed.

Upon substituting the values taken from Table III, we find an almost exact saturation of these relations.

Now we turn to a description of quantum correlations for the electromagnetic field in our fundamental state of the atom-field system. The second moments for the field variables are given in Table IV. These values of the correlations imply an almost complete decoupling between the corotating and counter-rotating modes, so that the uncertainty is almost saturated separately for each mode. The state of the field in the counter-rotating mode is a coherent state, but the state in the corotating mode is highly squeezed; the ratio of the correlation for the two quadratures Q_- and P_- is about 3.5×10^4. However, the fluctuations of the field are still small as compared to the field value $P_-^{\mathrm{eq}} = 1.5 \times 10^6$. The plots of the Wigner function in Figs. 7 and 8 illustrate the difference in quantum fluctuations between the counter-rotating and corotating modes.

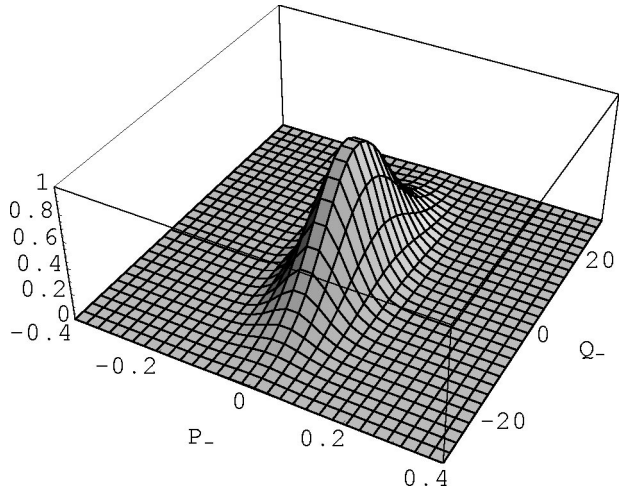

FIG. 8. The $Q_- - P_-$ cross section of the Wigner function. In this (corotating mode) the fluctuations of the electromagnetic radiation are strongly squeezed. Note the change of the scale, as compared to Fig. 7.

V. DISCUSSION

We have shown that the dynamical treatment of the relevant modes of the electromagnetic field enables one to reproduce exactly the properties of the Trojan states studied previously in the presence of a given, external wave. However, there appear features totally absent from previous studies, to our knowledge. First, the back reaction of the electron on the electromagnetic field causes a detuning from the exact resonance. As a result, the stability region now also covers the anti-Trojan states, that before were found to be classically unstable. Second, our analysis shows that, to achieve the equilibrium state of the mutually interacting atom-field system, we must take into account both polarization modes of the field: corotating and counter-rotating. The inclusion of only the corotating mode, as proposed in Ref. [10], is not sufficient to achieve an equilibrium state.

The quantization procedure adopted by us in this work consists of quantizing the corrections to the classical solution. These quantum corrections describe the shape of the electronic wave packet and the quantum fluctuations of the electromagnetic field around its classical value. The field fluctuations turn out to be significantly different for the two modes: for the counter-rotating mode the fluctuations are as for the vacuum state, whereas for the corotating mode they exhibit strong squeezing.

The choice of one particular solution from the class of equivalent classical solutions spontaneously breaks the rotational symmetry of the initial Hamiltonian. The method of quantization around the classical solution used here can also be applied to a similar problem of electronic Trojan states in a polar molecule [13]. In this case, the role of the electromagnetic field is played by the rotating molecular dipole. The application of our method would require a dynamical treatment of the relevant molecular degrees of freedom.

ACKNOWLEDGMENTS

We would like to thank Jan Mostowski for fruitful discussions, and we acknowledge the support from KBN Grant No. P03B0313.

[1] I. Bialynicki-Birula, M. Kaliński, and J. H. Eberly, Phys. Rev. Lett. **73**, 1777 (1994). An earlier prediction of such states based on a semiclassical approximation was made by H. Klar, Z. Phys. D: At., Mol. Clusters **11**, 45 (1989).
[2] D. Farrelly and T. Uzer, Phys. Rev. Lett. **74**, 1720 (1995).
[3] M. Kaliński, J. H. Eberly, and I. Bialynicki-Birula, Phys. Rev. A **52**, 2460 (1995).
[4] D. Delande, J. Zakrzewski, and A. Buchleitner, Europhys. Lett. **32**, 107 (1995); J. Zakrzewski, D. Delande, and A. Buchleitner, Phys. Rev. Lett. **75**, 4015 (1995).
[5] E. Lee, A. F. Brunello, and D. Farrelly, Phys. Rev. A **55**, 2203 (1997).
[6] C. Cerjan, E. Lee, D. Farrelly, and T. Uzer, Phys. Rev. A **55**, 2222 (1997).
[7] T. Uzer, E. Lee, D. Farrelly, and A. F. Brunello, Contemp. Phys. **41**, 1 (2000).
[8] Z. Bialynicka-Birula and I. Bialynicki-Birula, Phys. Rev. A **56**, 3623 (1997).
[9] D. Delande and J. Zakrzewski, Phys. Rev. A **58**, 466 (1998).
[10] M. A. Rippin and P. L. Knight, J. Mod. Opt. **43**, 807 (1996).
[11] M. Kaliński and J. H. Eberly, Phys. Rev. Lett. **77**, 2420 (1996).
[12] A. F. Brunello, T. Uzer, and D. Farrelly, Phys. Rev. Lett. **76**, 2874 (1996).
[13] H. A. Haus and Y. Lai, J. Opt. Soc. Am. B **7**, 386 (1990).
[14] I. Bialynicki-Birula and Z. Bialynicka-Birula, Phys. Rev. Lett. **77**, 4298 (1996).
[15] I. Bialynicki-Birula, Acta Phys. Pol. **29**, 3569 (1998).